New Application Technique for Gold Deposited Mylar Film

Steven R. Mart, Stephen T. McClain
Mechanical Engineering Department
Baylor University

Abstract

Gold deposited Mylar film is commonly used to establish a constant heat flux convective boundary condition for wind-tunnel test surfaces. To minimize conduction through the test plate and promote a constant flux boundary, the accepted technique for mounting Mylar film to a surface is to apply the film oriented as gold-side up. However, the accepted mounting technique causes problems if the films are used to explore convective heat transfer from surfaces with high thermal conductivity protuberances and surface roughness. If high thermal conductivity elements are attached to the side with the gold layer, the local resistance of the film is lowered and hotspots with local increases in heat generation are created. To overcome the problems with roughness-element attachment, a new technique for mounting gold-deposition Mylar film in a gold-side down orientation was developed. This new application technique allows for the roughness elements to be mounted to the plastic side of the film while ensuring that the heat generation from the gold-deposition side is not disrupted. However, with this inverted mounting orientation, conduction into the test plate and conduction through the Mylar film must be considered when determining local convection coefficients. To validate measurements of convection coefficients made using the Mylar film and the new application technique, a series of test measurements has been performed using spherical segment roughness elements applied to a heated vertical test plate in natural convection. The temperature distributions of both sides of the test plate were measured using an infrared camera. The resulting unperturbed convection coefficients and the protuberance fin efficiencies are in general agreement with classical correlations for the test situations.

Introduction

Gold deposited Mylar film is used to apply a known constant flux boundary condition for convective heat transfer studies. The technique has been commonly used for gas turbine applications and for the study the heat transfer from ice accretion roughness[1]. When surface temperatures are measured using thermochromic crystals[1] or infrared thermometry[2], the results can be used to determine local heat transfer variations along the surface of the Mylar film.

Icing is a serious flight safety concern because it not only adds additional weight to an aircraft but also disrupts and alters the fluid flow over the aircraft. Flow disruption can decrease lift, stall angle of attack, stability and efficiency while increasing the chance of stalls or pitch-overs. In order to compensate for these factors, the amount of lift generated by the aircraft must be increased. Increased lift can be achieved by either increasing the velocity at which the aircraft is traveling or increasing its angle of attack[3]. When flying at high altitudes, the velocity can be increased, generating the necessary increase in lift. However, when an aircraft is landing, its velocity must be reduced so that it can land safely. Therefore, the angle of attack at which the plane is flying must be increased. This makes the presence of any ice accumulation on an aircraft's body incredibly

dangerous since the lift demands required for the safe landing of a clean aircraft (one without any ice accumulation) are so high. The additional increase in angle of attack needed to compensate for ice accumulation can prematurely induce flow separation off the control surfaces of the aircraft, resulting in what is known as a stall. Upon stalling, the lift generated by the aircraft drops dramatically and can potentially cause the aircraft to crash[4].

Given the inherent dangers of icing and given the need to predict and counteract ice accumulation, research has already been performed on iced airfoil heat transfer since the local roughness element heat transfer coefficients are critical to the development of ice protuberances. The first attempt to understand the heat transfer of a scale roughness element was performed by Henry et al.[5]. Their data showed that the local heat transfer at the elements was enhanced for laminar flow but that enhancement diminished greatly once the flow became turbulent. Using infrared cameras, they measured the temperature across plastic, spherical segments mounted on a thin plate in an established fluid flow. However, in order to simplify experimentation, Henry et al. made two critical assumptions: conduction through their plate was negligible and radiation from the surface to the ambient was negligible. However, in 2007, McClain et al.[6] demonstrated that 1) these two effects were important and 2) because the plate used by Henry et al.[5] was heated using infrared lamps with an unknown heat flux, the two separate effects could not be isolated.

To expand upon the research of Henry et al.[5], a thin plate with simulated ice accumulation will be mounted in the Baylor University Subsonic Wind-Tunnel to establish it in a controlled airflow. Using a constant flux heating source constructed from gold deposited Mylar film to heat the roughness elements, the local surface temperature across the plate and "ice" will be measured using an infrared camera. Finally, the acquired data will be used to analyze how the size, height, and material properties of the roughness elements affected the heat transfer coefficient.

Due to the high thermal conductivity protuberances and surface roughness that needed to be mounted to the Mylar film, traditional application methods of the film are no longer applicable. The application of these high conductivity elements to the gold side of the Mylar film causes a reduction in the local resistance of the film generating a hot spot and negating the constant heat flux created by the Mylar. In order to avoid this problem, the Mylar was mounted gold-side down. This new orientation allowed for the roughness elements to be mounted to the non-conductive plastic side of the film ensuring that the resistance of the gold-side was undisturbed. While this flipped orientation calls for the consideration of conduction through the Mylar and the Plexiglas plate, experimentation using the high conductivity roughness elements discussed earlier yielded convection coefficients and protuberance fin efficiencies that agree with classically accepted values. The purpose of this investigation is to apply the new Mylar heater construction technique and evaluate the validity of measurements made using the Mylar test piece and infrared thermometry measurements of the surface temperature. Once the method is tested on a small scale (in this study), the final intent of the investigation is to explore the details of the local convective heat transfer coefficients during the beginning of icing on aircraft surfaces on a larger flat plate installed in the Baylor University Subsonic Wind-Tunnel. Methods to determine local convection coefficients on the protuberances on the small test piece of this study will also be explored.

Experimental Methodology

The deposition of a thin gold layer onto a Mylar sheet creates an electrically conductive layer that can be used to create a constant flux heat transfer boundary condition. However, to study the effects of protuberance thermal conductivity on the local heat transfer coefficients, elements with varying thermal conductivity must be attached to a heated surface. Since high values of thermal conductivity usually correlate to high values of electrical conductivity, elements with high thermal conductivity cannot be directly connected to the gold layer of a Mylar deposited sheet. If highly conductive elements are connected to the gold layer, the parallel resistances will lower the local resistance to electricity and create hot spots or areas of varying heat flux on the Mylar deposited sheet. To avoid hot spots, a new test piece construction method was developed. The following sections present the traditional test piece construction technique and the revised construction technique. The experimental procedure and data reduction equation for the heat transfer coefficient evaluation based on electrical power consumption and surface temperature measurements are also presented.

Traditional Mylar Application Method

Traditional construction of test plates using gold deposited Mylar film orients the film gold-side up[7]. This construction is achieved by first measuring and cutting the film to the appropriate size needed to mount to the Plexiglas being used, making sure that the gold side of the Mylar is not scratched or touched as the gold is very fine and susceptible to degradation. Anywhere that the gold has been touched or scuffed should be considered damaged and unsuitable for use. Then, using masking tape to cover the areas of the Plexiglas plate that will not be covered with Mylar, a spray is used to apply an even layer of adhesive to the area of Mylar film application. After the adhesive has been applied, the film is carefully aligned, mounted to the test plate, and the masking tape is removed. Using a soft to medium hardness rubber brayer, a light pressure is applied to the film in several even passes over the surface of the foil, starting in the middle and moving outwards. After application of the foil, copper tape is adhered to the Plexiglas next to the edges of the film perpendicular to the leading edge of the test piece, leaving approximately 1/16 inch between the foil and the tape. Several inches of tape should be allowed to extend off one end of the plate. Then, silver conductive paint is liberally applied along the inner edges of the copper tape and the Mylar, filling the 1/16 inch gap left between the two materials. The silver paint should overlap both the Mylar and the copper tape by approximately 1/16 inch to 1/8 inch. After applying the paint, a 12 inch piece of 18 gauge copper wire is soldered to the ends of each piece of copper tape extending off the plate.

New Mylar Application Method

The construction of a plate using the new application method starts similarly to the traditional method. The Mylar is cut in the same manner, using the same caution not to touch or scratch the film. As in the original method, masking tape is applied to the non-Mylar covered Plexiglas portions of the test plate, but the Mylar covered area of the plate is reduced by ¼ inch on the 2 sides that would normally have copper tape applied next to them. Spray adhesive is applied to the plate and the masking tape is removed. The Mylar is then carefully adhered gold-side down, leaving ¼ inch of Mylar unglued on each side. The orientations of the different layers of the test piece are illustrated below in Figure 1. After using the brayer to ensure that there is a good contact between the glue and the Mylar, the unglued ends of the Mylar are gently lifted and a piece of copper tape is adhered to the Plexiglas underneath each side, leaving half of the tape under the Mylar and half exposed to the air. Again, several inches of tape should extend off of the plate. The unglued ends of

the Mylar are carefully lifted again and conductive silver paint is applied to the top of the copper tape and any other unglued area underneath the Mylar. Doing this will ensure that there is a good contact between the copper tape and the Mylar. The silver paint is also acting as an adhesive used to glue the remaining ends of the Mylar to the plate. Finally, copper wire is then soldered to the copper tape following the same method described in the traditional application process.

Protuberance Attachment

Once the test plate is constructed, the high conductivity spherical roughness elements need to be attached to the Mylar. These protuberances are created from spherical thermoplastics intended for cervical decoration (necklace beads) purchased from a regional hobby retail distributor. Given the original intent of these thermoplastics, each element has a small cylindrical cavity extending through its center.

To attach the protuberances to the test plate, the thermoplastics are first fabricated into hemispheres. To accomplish this, each sphere is gently sanded with a medium roughness sand paper until a symmetrical hemisphere is formed. These hemispheres are then fastened to the center of the Mylar with a light layer of cyanoacrylate brush on adhesive applied to the bottom of each protuberance. Once the elements are applied, a light even layer of flat black spray paint is applied to the surface of the plate to reduce reflected emissions and create a constant surface emission. The complete construction of the test apparatus can be seen below in Figure 2.

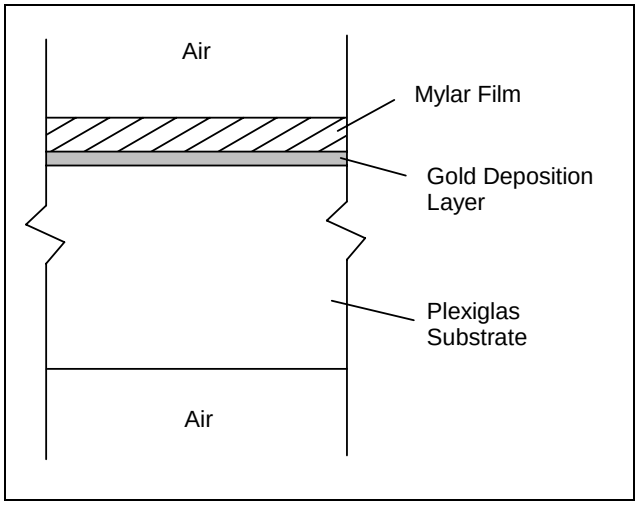

Figure 1: New Test Plate Construction

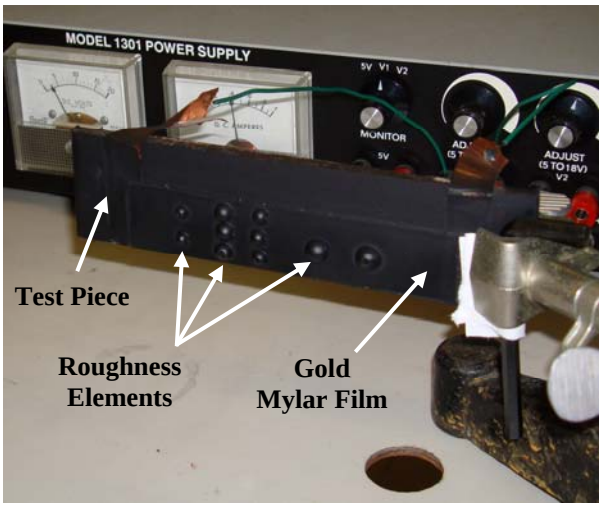

Figure 2: Sample Test Apparatus

Experimental Measurements

After the test apparatus construction is completed and the paint allowed ample time to dry, the plate is securely mounted horizontally on a test stand, approximately 3 inches off the testing surface. The roughness elements are positioned so they are facing towards the infrared camera and the mounting grips on the test stand are only contacting the Plexiglas to keep electrical conduction to a minimum. The wire leads of the test plate are connected to a power supply and the power supply dials for current and voltage are set to their lowest settings. Once the test plate is secured, the infrared camera is positioned 9 ½ inches in front of the test plate. The infrared camera is then turned on and the power supply adjusted to 4.5V at 0.5A. After allowing the surface temperature of the plate to reach steady-state, the temperature of the front surface is recorded with the infrared camera and the

temperature of the back surface is measured using an infrared gun. To minimize any radiative effects from the lights within the room, these measurements are taken at room temperature in a dark room. Figure 3 demonstrates the experimental setup for the test measurements.

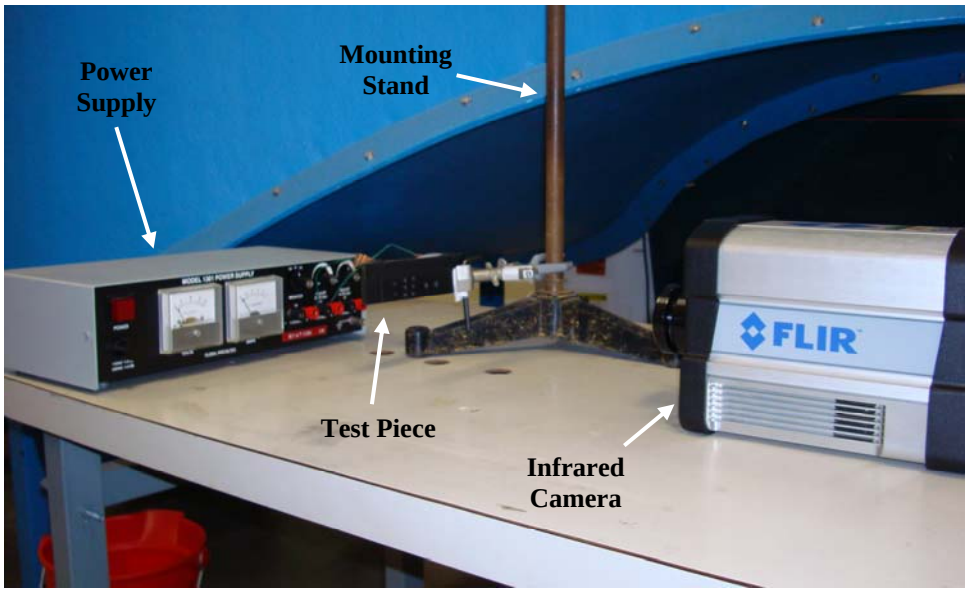

Figure 3: Validation Setup Using Infrared Camera

Data Reduction

Based on the new construction method, the added resistance of the Mylar film and its relation to the Plexiglas plate must be considered in the reduction of the experimental data. The thermal resistance circuit for the test apparatus can be seen in Figure 4. The development of the data reduction equation begins by applying Fourier's Law of Conduction to express the temperature of the gold layer of the Mylar in terms of the measured temperatures of the Plexiglas surface and the Mylar surface. From the Mylar surface, the temperature of the gold layer is:

$$T_g = T_M + \frac{q''_M t_M}{k_M} \tag{1}$$

where T_M is the local Mylar surface temperature measured using the infrared camera, q''_M is the flux through the Mylar, t_M is the thickness of the Mylar film, and k_M is the thermal conductivity of the Mylar. Similarly, the temperature of the gold layer in terms of the Plexiglas surface temperature is:

$$T_g = T_P + \frac{q''_P t_P}{k_P} \tag{2}$$

where T_P is the Plexiglas surface temperature measured using the infrared thermometer, q''_P is the flux through the Plexiglas, t_P is the thickness of the Plexiglas plate, and k_P is the thermal conductivity of the Plexiglas.

$$T_g = T_P + \frac{\left(\frac{\dot{W}_E}{A} - q''_M\right) t_P}{k_P} \tag{3}$$

Equating (1) and (3) for the temperature of the gold layer yields:

$$T_M + \frac{q''_M t_M}{k_M} = T_P + \frac{\left(\frac{\dot{W}_E}{A} - q''_M\right) t_P}{k_P} \qquad (4$$

To determine the convection coefficient, the flux through the Mylar in Equation (4) must be expressed in terms of the convective flux at the Mylar surface. However, at the Mylar surface there is a combination of convection, radiation, and lateral conduction. That is,

$$q''_M = h_M \left(T_M - T_\infty\right) + \varepsilon\sigma\left(T_M^4 - T_w^4\right) + k_M \left(\left.\frac{dT_M}{dn}\right|_s\right) \qquad (5)$$

where h_M is the convective heat transfer coefficient, T_∞ is the temperature of the air far from the heated surface, ε is the emissivity of the Mylar surface, and σ is the Stefan-Boltzman constant. Substituting (5) into (4) and solving for the convection coefficient yields

$$h_M = \left(\frac{\frac{\dot{W}_E}{A}\frac{t_P}{k_P} - \left(T_M - T_P\right)}{\left(T_M - T_\infty\right)}\right)\left(\frac{t_M}{k_M} + \frac{t_P}{k_P}\right)^{-1} - \frac{\varepsilon\sigma\left(T_M^4 - T_w^4\right) + k_M\left(\left.\frac{dT_M}{dn}\right|_s\right)}{\left(T_M - T_\infty\right)} \qquad (6)$$

Preliminary Results with Test Apparatus

Measurements of the test apparatus were taken for a preliminary investigation of the validity of the test apparatus construction and data reduction methods. Two aspects of the test apparatus and method were examined. First, the convection coefficients on the regions on the test apparatus that were unperturbed with elements were compared to traditional correlations for vertical surfaces in natural convection. Second, methods to investigate the heat transfer coefficients on the protuberance surfaces were investigated. The results of the two investigations follow.

Vertical Plate Results

Figure 5 presents the temperature measurements from the infrared camera during the preliminary investigation. The temperature measurements of Figure 5 were then reduced based on the other experimental measurements using Equation (6). The resulting heat transfer coefficients are reported in Figure 6. As seen in Figure 6, there is a low variation of the convection coefficient in the unperturbed central region of the plate. For the central 2/3 of width and central 1/3 of height of test apparatus, there is only a 3.9% variation in the convective heat transfer coefficient of approximately 22 W/(m^2·K). The small size of the apparatus and these small variations indicates that the new Mylar orientation will provide minimal variations in heat flux on the larger wind-tunnel test apparatus.

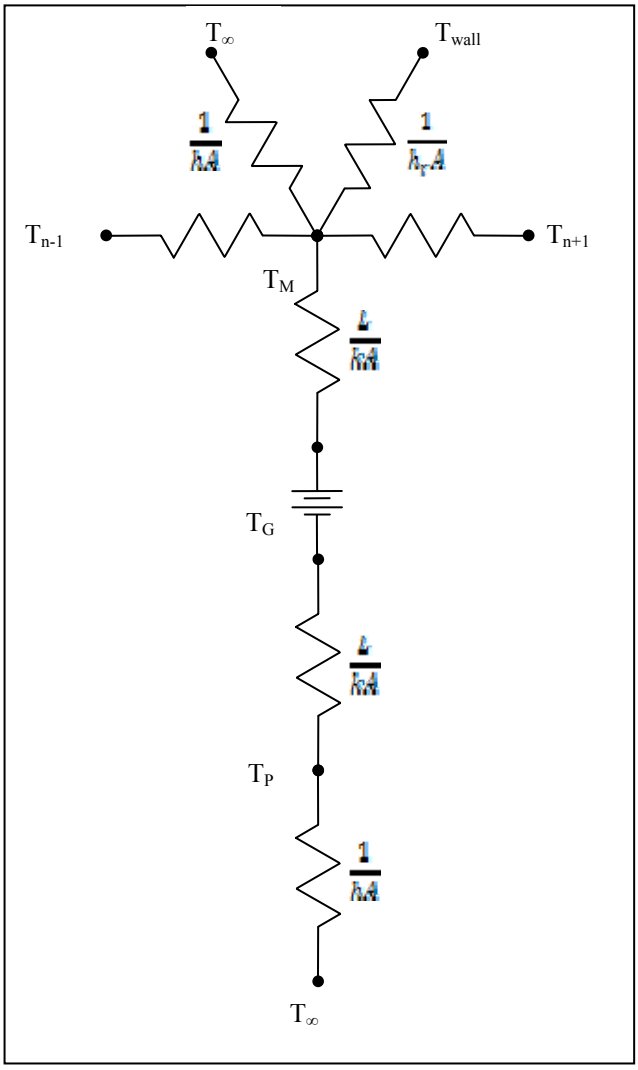

Figure 4: Thermal Resistance Circuit for New Test Piece Construction

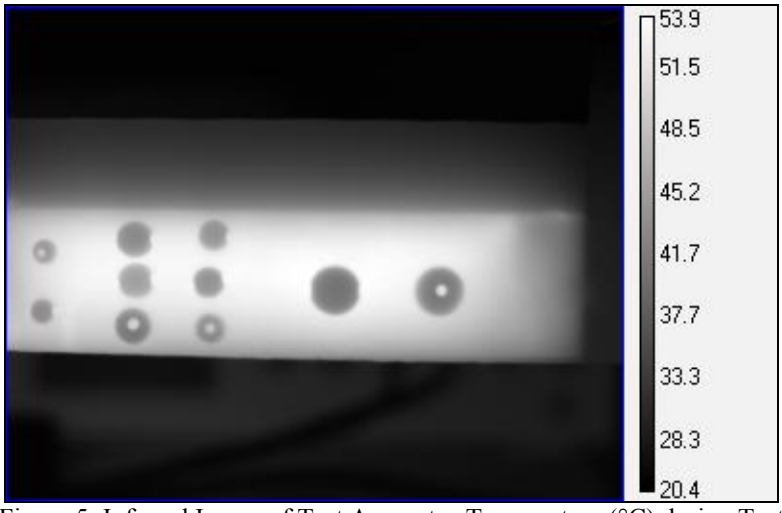

Figure 5: Infrared Image of Test Apparatus Temperature (°C) during Test

To validate the preliminary test results, the unperturbed convection coefficients were compared to classical correlations for natural convection from a vertical heated surface. For free convection on a vertical plate, the Rayleigh number can be found by

$$Ra_L = \frac{g\beta(T_s - T_\infty)L^3}{\nu\alpha} \tag{7}$$

where g is the gravitational constant, β is the volumetric thermal expansion coefficient, T_s is the surface temperature, T_∞ is the ambient temperature, and ν and α are the kinematic viscosity and thermal diffusivity, respectively[8]. Churchill and Chu proposed two correlations to find the local average Nusselt number for a given Rayleigh number[9]. The first provides the average Nusselt number over the entire range of Rayleigh numbers given by the equation

$$\overline{Nu}_L = \left\{ 0.825 + \frac{0.387 Ra_L^{1/6}}{\left[1 + (0.492/Pr)^{9/16}\right]^{8/27}} \right\}^2 \tag{8}$$

And the second provides the average Nusselt number for laminar flow ($Ra \leq 10^9$)

$$\overline{Nu}_L = 0.68 + \frac{0.670 Ra_L^{1/4}}{\left[1 + (0.492/Pr)^{9/16}\right]^{4/9}} \tag{9}$$

Using the values of the Nusselt number given by the previous two equations, the average convective heat transfer coefficient can be found by the equation

$$\overline{Nu}_L = \frac{\bar{h}L}{k} \tag{10}$$

where L is the vertical length and k is the thermal conductivity. After applying both correlations of Churchill and Chu, the average convective heat transfer coefficient was found to be 8.13 [W/(m^2·K)] and 8.73 [W/(m^2·K)], respectively.

Interestingly, the experimentally measured unperturbed convection coefficients are approximately three times the values predicted by the correlations of Churchill and Chu. However, two phenomena provide reasonable explanations for the difference. First, power losses or power dissipation in the lead wires and connections to the gold layer were not evaluated. For the preliminary measurements, the power through the plate was not measured directly. The power was calculated from the voltage and current measurements from the power supply used for experimentation. Therefore, if there was any power loss or power dissipation through the wires and plate connection, it was unaccounted for and the actual power consumed by the gold layer is less than the power generated by the voltage supply. Second, the measurements were not made in a concealed chamber. The measurements were made with the test apparatus exposed in a laboratory with ventilation. Because of the ventilation currents in the room, a true natural convection situation cannot be confirmed for the preliminary measurements. Eliminating both of these effects would lead to lower heat transfer coefficients than those calculated based on the assumed power consumption. While agreement with the correlations is less than desired, the experimentally measured values of convection coefficients in the center section of the plate are certainly in-line with values expected for gases in natural convection[8].

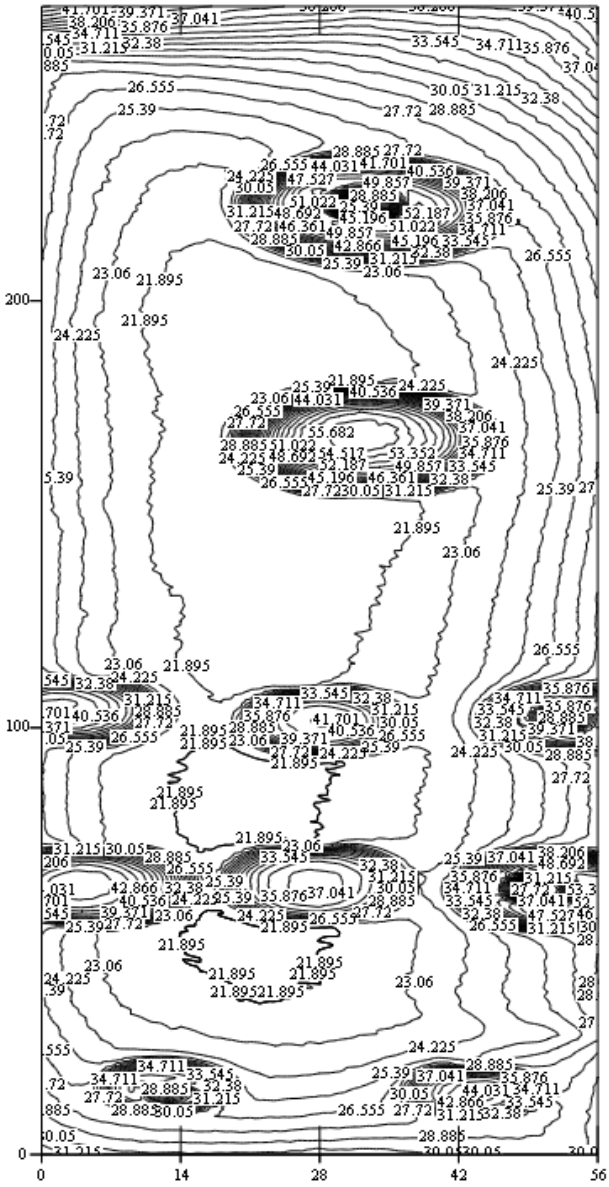

Figure 6: Convection Coefficients [W/(m^2·K)] on Test Piece With Plastic Elements

Fin Analysis Results

As seen in Figure 6, the calculated heat transfer coefficients along the protuberances were much greater than those of the unperturbed regions due to the fin like nature of these elements. However, along the protuberances, Equation (6) is not valid. Because the protuberances are extended surfaces or "fins", they lose heat radially near the bases of each protuberance. As such, the remaining heat flux along the heights of the protuberances is not equal to the power flux from the gold foil.

Treating the protuberances as fins allows an inverse technique for evaluating the average heat transfer coefficients on the protuberances. The slender fin equation, Equation (11), may be used to predict temperature variations along the protuberances

$$\frac{d^2T_R}{dy^2}+\frac{1}{A}\frac{dA}{dy}\frac{dT_R}{dy}-\frac{h_d\left(T_R-T_f\right)}{k_R A}\frac{dA_s}{dy}-\frac{q_r''}{k_R A}\frac{dA_s}{dy}=0 \tag{11}$$

with the boundary conditions

$$T_R(y=0)=T_w \text{ and } \left.\frac{dT_R}{dy}\right|_{y=0}=-\frac{VI}{A_{Au}}\frac{A_f}{k_R}$$

After normalizing the fin equation, it takes the form

$$\frac{d^2\theta_R}{dy^2}+\frac{1}{A}\frac{dA}{dy}\frac{d\theta_R}{dy}-\frac{1}{k_R A}\frac{dA_s}{dy}\left[h_d\left(\theta_R-\theta_f\right)\right]=0 \tag{12}$$

where the normalized temperatures, θ_R and θ_f, are defined as

$$\theta_R=\frac{T_R-T_\infty}{T_w-T_\infty} \text{ and } \theta_f=\frac{T_f-T_\infty}{T_w-T_\infty} \tag{13}$$

and the boundary conditions become

$$\theta_R(y=0)=1 \text{ and } \left.\frac{d\theta_R}{dy}\right|_{y=0}=-\frac{VI}{A_{Au}}\frac{A_f}{k_R\left(T_w-T_\infty\right)}$$

Figure 7 presents the normalized temperature of the largest protuberance shown in Figure 5 (center of the IR image) as a function of the normalized height from the unperturbed elevation. The inverse method involves integrating the normalized fin equation, Equation (12), by iteratively assuming a value for the average convection coefficient. The resulting estimate of the protuberance convection coefficient would be the value of the assumed convection coefficient that minimizes the error between the integrated temperature profile and the measured temperature profiles.

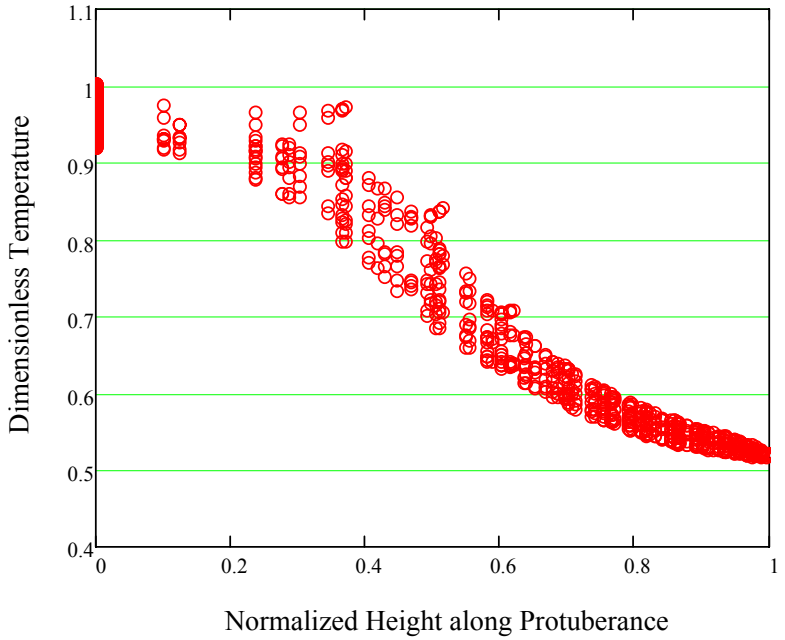

Figure 7: Normalized Temperature Variation along the Height of the Protuberance

Because of the issues noted in the unperturbed convection coefficient investigation, the preliminary fin investigations are incomplete. In addition to the previously noted issues, the thermal conductivity of the plastic beads is also unknown. Until the issues with the unperturbed surface convection coefficients are resolved and until the thermal conductivity and uniformity of the plastic beads is known, the protuberance fin analysis must wait.

Conclusions

Through experimentation and observation, the new mounting method for gold deposited Mylar was determined to be a viable solution for the mounting of high thermal conductivity elements. The flipped orientation of the gold ensures that the constant flux boundary condition of the film is maintained while still providing valid measurements and temperatures when evaluated with infrared thermometry. The preliminary results are encouraging, but issues with the electrical measurements and heat transfer configuration caused the convection coefficient measurements to vary considerably from traditional natural convection correlations. Future experimentation should include the consideration of power wires and electrical connections to the plate. To better validate the method, a new test apparatus will be installed in a wind-tunnel to compare the results to a more repeatable forced convection boundary layer configuration. This new test apparatus will also replicate the initial stages of ice accumulation on an aircraft so the local convective heat transfer coefficients may be evaluated. Finally, to further explore the heat transfer on the protuberances, the thermal conductivity of the protuberances must be determined.

Acknowledgements

The authors thank Dr. William Jordan and the Mechanical Engineering Department at Baylor University for their support of these activities.

Nomenclature

h_M	=	convective heat transfer coefficient [W/(m^2·K)]
k_M	=	thermal conductivity of the Mylar [W/(m·K)]
k_P	=	thermal conductivity of the Plexiglas [W/(m·K)]
$\overline{Nu_L}$	=	average Nusselt number
Pr	=	Prandtl number of air at film temperature
q''_M	=	flux through the Mylar (W/m^2)
q''_P	=	flux through the Plexiglas (W/m^2)
T_G	=	temperature of the gold deposition layer (K)
T_M	=	local Mylar surface temperature (K)
T_P	=	Plexiglas surface temperature (K)
T_s	=	surface temperature (K)
T_∞	=	temperature of the air far from the heated surface (K)
g	=	gravitational constant (m/s^2)
t_M	=	thickness of the Mylar film (m)
t_P	=	thickness of the Plexiglas plate (m)
α	=	thermal diffusivity of air at film temperature (m^2/s)

β = volumetric thermal expansion coefficient (1/K)
ε = emissivity of the Mylar surface
ν = kinematic viscosity of air at film temperature (m^2/s)
σ = Stefan-Boltzman constant [$W/(m^2 \cdot K^4)$]

References

1. Baughn, J. W., Hoffman, M. A., and Makel, D. B., "Improvements in a new technique for measuring and mapping heat transfer coefficients," *Review of Scientific Instruments*, Vol. 57, No. 4, April 1986.
2. Dukhan, N., "Measurement of the Convective Heat Transfer Coefficient from Ice Roughened Surfaces in Parallel and Accelerated Flows" Ph.D. Dissertation, University of Toledo, December 1996.
3. Gent, R. W., Dart, N. P., and Cansdale, J. T., "Aircraft Icing", *Philosophical Transactions of the Royal Society*, Vol. 358, pg 2873-2911, 2000.
4. Reinmann, J. J, "Icing: Accretion, Protection, Detection", *AGARD Lecture Series 197 'Flight in an Adverse Environment'*, November 1994.
5. Henry, R. C., Hansman, R. J., Breuer, K. S., "Heat Transfer Variation on Protuberances and Surface Roughness Elements", *Journal of Thermophysics and Heat Transfer*, vol 9, No. 1, March 1995.
6. McClain, S. T., Vargas, M., Kreeger, R. E., and Tsao, J.-C., "Heat Transfer from Protuberances," *Journal of Thermophysics and Heat Transfer*, Vol. 21, No. 2, pg 337-345, 2007.
7. Byerley, Dr. A., Wolf, Capt. J., "Building Heat Transfer Models and Painting Liquid Crystals", Instructional Video, April 2002.
8. Incropera, F., Dewitt, D., Bergman, T., Lavine, A., *Fundamentals of Mass and Heat Transfer*, John Wiley & Sons, Inc, Hoboken, NJ, pp. 571, 2007.
9. Churchill, S. W., and H. H. S. Chu, "Correlating Equations for Laminar and Turbulent Free Convection from a Vertical Plate," *Int. J. Heat Mass Transfer*, 18, 1323, 1975.

STEVEN R. MART
Steven is a senior mechanical engineering student at Baylor University and will be graduating in May of 2009. He is currently performing research on the accretion of ice on aircraft surfaces and hopes to continue his research this fall in graduate school.

STEPHEN T. MCCLAIN
Dr. Stephen T. McClain is an Assistant Professor of Mechanical Engineering at Baylor University. Dr. McClain received his B.S. in mechanical engineering from The University of Memphis in 1995, and he received his M.S. (1997) and Ph.D. (2002) degrees in mechanical engineering from Mississippi State University. Dr. McClain's primary research areas are heat transfer and aerodynamics of turbine blades and components, energy systems design, and in-flight ice accretion on aircraft surfaces and engine components.